



RCSI

UNIVERSITY
OF MEDICINE
AND HEALTH
SCIENCES

Royal College of Surgeons in Ireland

repository@rcsi.com

Unilateral hippocampal CA3-predominant damage and short latency epileptogenesis after intra-amygdala microinjection of kainic acid in mice.

AUTHOR(S)

Genshin Mouri, Eva Jimenez-Mateos, Tobias Engel, Mark Dunleavy, Seiji Hatazaki, Alexia Paucard, Satoshi Matsushima, Waro Taki, David Henshall

CITATION

Mouri, Genshin; Jimenez-Mateos, Eva; Engel, Tobias; Dunleavy, Mark; Hatazaki, Seiji; Paucard, Alexia; et al. (2008): Unilateral hippocampal CA3-predominant damage and short latency epileptogenesis after intra-amygdala microinjection of kainic acid in mice.. Royal College of Surgeons in Ireland. Journal contribution. <https://hdl.handle.net/10779/rcsi.10789970.v2>

HANDLE

[10779/rcsi.10789970.v2](https://hdl.handle.net/10779/rcsi.10789970.v2)

LICENCE

CC BY-NC-ND 4.0

This work is made available under the above open licence by RCSI and has been printed from <https://repository.rcsi.com>. For more information please contact repository@rcsi.com

URL

https://repository.rcsi.com/articles/journal_contribution/Unilateral_hippocampal_CA3-predominant_damage_and_short_latency_epileptogenesis_after_intra-amygdala_microinjection_of_kainic_acid_in_mice_/10789970/2

available at www.sciencedirect.comwww.elsevier.com/locate/brainres**BRAIN
RESEARCH**

Research Report

Unilateral hippocampal CA3-predominant damage and short latency epileptogenesis after intra-amygdala microinjection of kainic acid in mice

Genshin Mouri^{a,b,1}, Eva Jimenez-Mateos^{a,1}, Tobias Engel^a, Mark Dunleavy^a,
Seiji Hatazaki^{a,b}, Alexia Paucard^a, Satoshi Matsushima^b, Waro Taki^b, David C. Henshall^{a,*}

^aDepartment of Physiology and Medical Physics, Royal College of Surgeons in Ireland, 123 St. Stephen's Green, Dublin, 2, Ireland

^bDepartment of Neurosurgery, Mie University School of Medicine, Mie, Tsu, Japan

ARTICLE INFO

Article history:

Received 18 March 2008

Keywords:

Epileptogenesis

FluoroJade B

Gliosis

Hippocampal sclerosis

Mossy fiber sprouting

Status epilepticus

ABSTRACT

Mesial temporal lobe epilepsy is the most common, intractable seizure disorder in adults. It is associated with an asymmetric pattern of hippocampal neuron loss within the endfolium (hilus and CA3) and CA1, with limited pathology in extra-hippocampal regions. We previously developed a model of focally-evoked seizure-induced neuronal death using intra-amygdala kainic acid (KA) microinjection and characterized the acute hippocampal pathology. Here, we sought to characterize the full extent of hippocampal and potential extra-hippocampal damage in this model, and the temporal onset of epileptic seizures. Seizure damage assessed at four stereotaxic levels by FluoroJade B staining was most prominent in ipsilateral hippocampal CA3 where it extended from septal to temporal pole. Minor but significant neuronal injury was present in ipsilateral CA1. Extra-hippocampal neuronal damage was generally limited in extent and restricted to the lateral septal nucleus, injected amygdala and select regions of neocortex ipsilateral to the seizure elicitation side. Continuous surface EEG recorded with implanted telemetry units in freely-moving mice detected spontaneous, epileptic seizures by five days post-KA in all mice. Epileptic seizure number averaged 1–4 per day. Hippocampi from epileptic mice 15 days post-KA displayed unilateral CA3 lesions, astrogliosis and increased neuropeptide Y immunoreactivity suggestive of mossy fiber rearrangement. These studies characterize a mouse model of unilateral hippocampal-dominant neuronal damage and short latency epileptogenesis that may be suitable for studying the cell and molecular pathogenesis of human mesial temporal lobe epilepsy.

© 2008 Elsevier B.V. All rights reserved.

1. Introduction

Mesial temporal lobe epilepsy (MTLE) is the most common and intractable seizure disorder in adults (Chang and Lowenstein,

2003; Engel, 2001). The causal factors in the pathogenesis of 48 human MTLE remain unknown. Its most common pathological 49 hallmark is asymmetric hippocampal neuron loss within the 50 endfolium (hilus and CA3) and CA1, with relative sparing of the 51

* Corresponding author. Fax: +353 1 402 2447.

E-mail address: dhenshall@rcsi.ie (D.C. Henshall).

Abbreviations: CA, cornu ammonis; DAPI, 4',6-diamidino-2-phenylindole; EEG, electroencephalogram; FjB, FluoroJade B; GFAP, glial fibrillary acidic protein; KA, kainic acid; LSN, lateral septal nucleus; MTLE, mesial temporal lobe epilepsy; NeuN, neuron-specific nuclear protein; NPY, neuropeptide Y

¹ These authors contributed equally to this work.

52 dentate granule neurons and CA2 subfield (Mathern et al., 1997;
 53 Meldrum and Bruton, 1992; Najm et al., 2006). Extra-hippocampal
 54 neuron loss within cortical regions and amygdala have been
 55 reported in some (Du et al., 1993; Hudson et al., 1993; Pitkanen
 56 et al., 1998), but not all (Bothwell et al., 2001; Dawodu and Thom,
 57 2005) clinical studies. Acutely-incurred damage following status
 58 epilepticus (SE) in patients is found within hippocampus, amyg-

59 dala, thalamic nuclei and piriform and entorhinal cortices (De-
 60 Giorgio et al., 1992; Fujikawa et al., 2000).

61 Convulsive SE in rodents has been used extensively to model
 62 seizure-induced neuronal death and MTLE pathology (Morimoto
 63 et al., 2004). In rats, systemic pilocarpine or kainic acid (KA) are
 64 most commonly used, but produce bilateral and widespread
 65 extra-hippocampal damage with limited or variable hippocampal

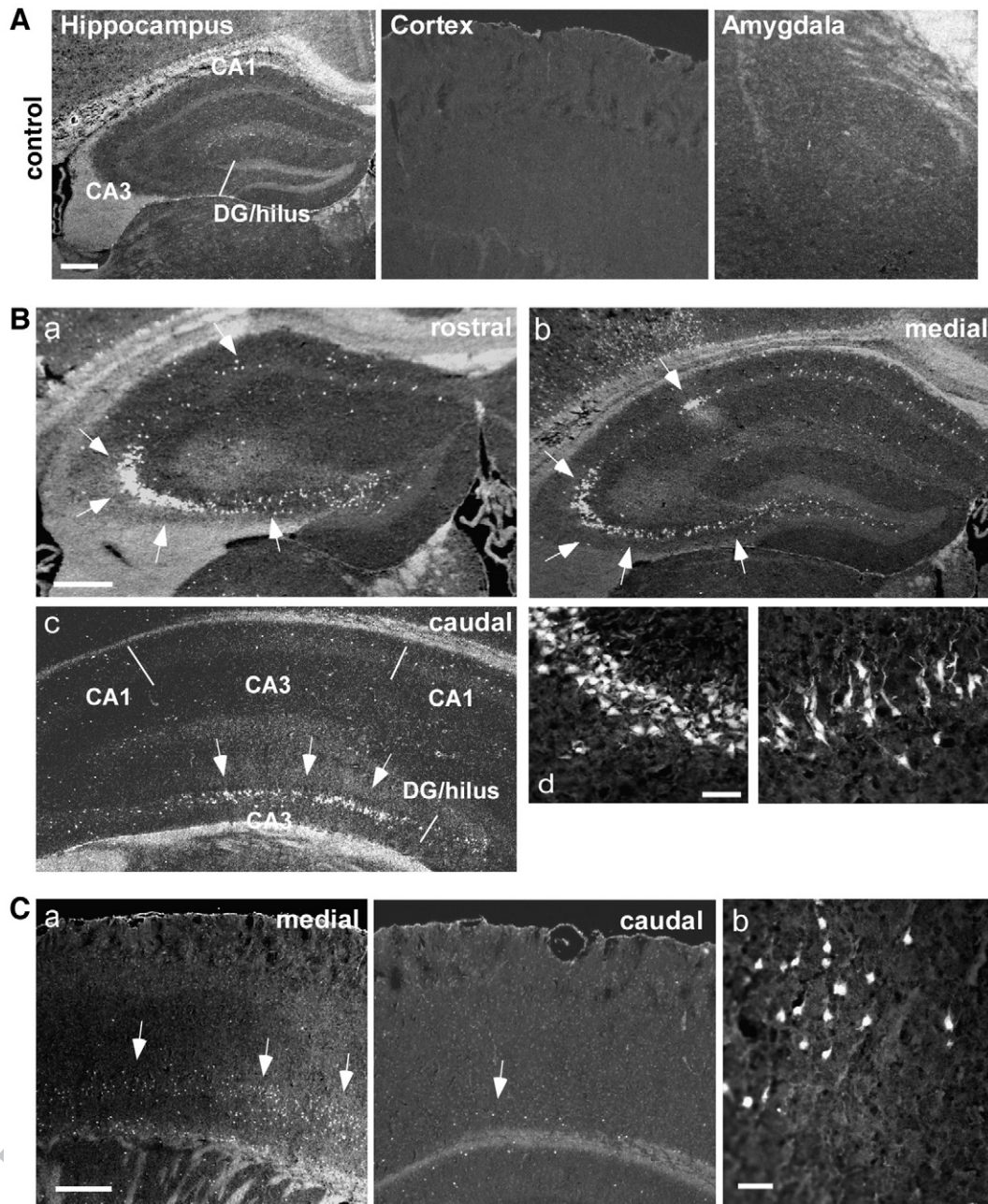


Fig. 1 – Hippocampal and cortical injury following seizures evoked by intra-amygdala KA microinjection. Photomicrographs show representative FluoroJade B (FjB) staining of ipsilateral fields from control and KA-treated mice at 24 h. (A) Staining (4X lens) in control mice for the hippocampus, cortex and amygdala. Note absence of FjB positive cells. (B) Representative images of ipsilateral hippocampus from seizure-damaged mice at rostral (AP, -1.22 mm), medial (AP, -1.82) and caudal (AP, -2.92 mm) levels, respectively. Arrows highlight FjB positive cells. Images in d show higher power views (40X lens) of FjB-positive cells in CA3 from (left panel) middle and (right panel) caudal levels. (C) Representative images in a show seizure damage in ipsilateral temporal cortex at medial and caudal levels. Panel b is a higher power image (40X lens) of representative cells at the level of medial temporal cortex. Scale bars, A, Ba, Ca, 500 μ m; Bd, Cb, 50 μ m.

66 pathology (Sloviter, 2005; Sloviter et al., 2007). In contrast, focally-
 67 evoked seizures by electrical stimulation of the perforant path in
 68 rats or mice replicate closely the unilateral pathology of MTL
 69 (Harvey and Sloviter, 2005; Kienzler et al., 2006; Sloviter, 1983).

70 Intra-cerebral KA injection offers an alternate approach to
 71 focal elicitation of seizures and induction of epileptogenesis.
 72 This includes intra-hippocampal KA (Gouder et al., 2003;
 73 Vezzani et al., 1999) and evoking SE by intra-amygdala KA
 74 microinjection. In the latter case, the seizures produce a mainly
 75 unilateral hippocampal lesion with limited extra-hippocampal
 76 damage (Ben-Ari et al., 1980; Henshall et al., 2002a,b). This model
 77 has been adapted with similar results to cats (Tanaka et al., 1985)
 78 and baboons (Menini et al., 1980). In mice, hippocampal damage
 79 is also largely unilateral, with damage to hippocampal CA3 and
 80 the hilus and minor cell death in CA1 (Araki et al., 2002; Murphy
 81 et al., 2007; Shinoda et al., 2004a). Whether hippocampal
 82 pathology extends from septal (dorsal) to temporal (caudal)
 83 pole has not been fully explored, nor has the extent of extra-
 84 hippocampal damage.

85 Status epilepticus is also an effective experimental approach
 86 to trigger epileptogenesis, with spontaneous seizures emerg-
 87 ing in the subsequent days or weeks. Characteristic hippocampal
 88 changes implicated as causative factors include neuronal
 89 death, rearrangement of dentate granule neuron axons (mossy
 90 fibre sprouting) (Wuarin and Dudek, 1996), astrogliosis (Li et al.,
 91 2008) and neurogenesis (Parent et al., 1997). Unilateral intra-
 92 amygdala KA microinjection can precipitate epilepsy within

93 two weeks in rats and cats (Tanaka et al., 1988, 1985). Intra-
 94 cerebral recordings in mice three weeks after intra-amygdala
 95 KA microinjection have shown the insult is epileptogenic,
 96 with spontaneous seizures originating from the hippocampus
 97 (Li et al., 2008).

98 The purpose of the present study was to characterize the
 99 extent of hippocampal and extra-hippocampal damage following
 100 seizures evoked by intra-amygdala KA microinjection in mice,
 101 and to determine the onset time of subsequent spontaneous
 102 seizures. Our data show seizure damage in this model is prin-
 103 cipally unilateral and mainly confined to the hippocampus, and
 104 that the injury precipitates epilepsy after a short latent period.

105 2. Results 106

107 2.1. Behavior during seizures evoked by kainic acid 108

108 Mice showed normal activity immediately after KA microinjec-
 109 tion. Polyspike seizure EEG typically started 5–10 min later, with
 110 mice showing immobility. Mice began to develop continuous
 111 seizures after a further 20 min. These episodes were character-
 112 ized by immobility, followed by tail extension (Straub-tail). Whole
 113 body clonus, head bobbing and rearing and falling (mouse Racine
 114 scale 6) were also commonly observed. Short periods of tonic-
 115 clonic seizures with loss of posture and jumping also occurred
 116 during the seizures.

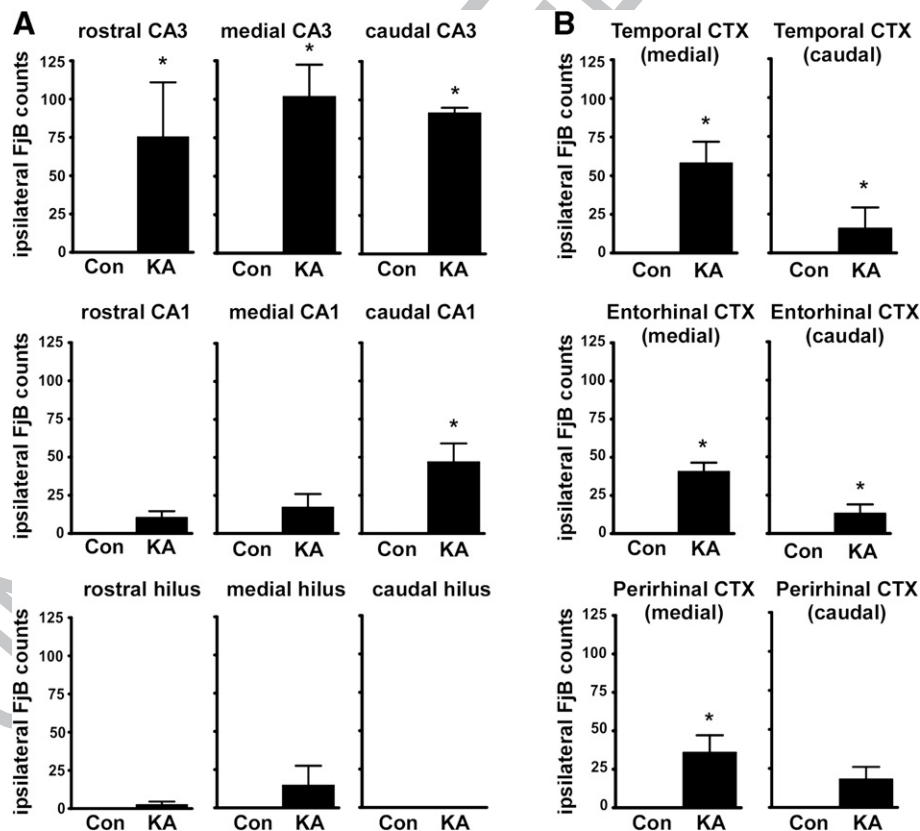


Fig. 2 – Quantification of seizure damage in ipsilateral hippocampus and cortex. (A) Graphs show mean FjB-positive cell counts at three stereotaxic levels for (top) CA3, (middle) CA1 and (bottom) hilus, in control (Con) and KA-treated mice (KA) at 24 h. (B) Graphs show FjB-positive cell counts in temporal, entorhinal and perirhinal cortex at two stereotaxic levels in control and KA-treated mice. Data are mean \pm SD from $n=4$ per group. * $p<0.05$ versus control.

117 2.2. Hippocampal damage following intra-amygdala KA 118 microinjection in mice

119 We recently described induction of seizures by intra-amygdala
120 KA microinjection in mice, seizure termination effects of two
121 anticonvulsants and hippocampal injury at the level of the
122 dorsal hippocampus (Shinoda et al., 2004a). In the present study
123 we sought to characterize the extent of hippocampal damage
124 and extra-hippocampal damage resulting from seizures evoked
125 by intra-amygdala KA microinjection, using FluoroJade B (FjB)
126 staining to mark irreversibly damaged cells. Four stereotaxic
127 levels were examined at 24 h, representing the level of KA
128 injection, and the rostral, medial (septal pole) and caudal
129 (temporal pole) extent of the hippocampus.

130 Control mice displayed no significant FjB staining in the
131 hippocampus ipsilateral or contralateral to the side of vehicle
132 injection (Figs. 1A,2A and data not shown). In contrast, mice
133 that received intra-amygdala KA microinjection had promi-
134 nent FjB staining in ipsilateral CA3 at the levels of the rostral,
135 medial and caudal hippocampus (Figs. 1B and 2A). Numbers of
136 FjB-positive CA3 cells in KA-injected mice were significantly
137 higher than controls at each level examined (Fig. 2A). Counts
138 in KA-injected mice were somewhat higher at medial and
139 caudal levels than rostral hippocampus (Fig. 2A). A variable
140 number of FjB-positive cells were present within the hilar
141 region of the dentate gyrus in these mice (Figs. 1B and 2A).

142 All KA-injected mice had small numbers of FjB-positive cells
143 present in ipsilateral CA1 at one or more of the three hippocampal

144 levels studied (Fig. 1B). Counts were only significant compared to
145 control at the level of caudal hippocampus (Fig. 2A). Occasional FjB-
146 positive cells were found within contralateral CA1 and CA3 in KA-
147 injected mice but numbers were not significant (data not shown).

148 2.3. Seizure damage in ipsilateral temporal, entorhinal and 149 perirhinal cortices

150 We next examined damage within three cortical regions at levels
151 corresponding to the medial and caudal hippocampus. No FjB-
152 positive cells were found in vehicle-injected controls (Figs. 1A
153 and 2B). Small but significant numbers of FjB-positive cells were
154 present in KA-injected mice in temporal, entorhinal and peri-
155 rhinal cortex at the level of medial hippocampus (Figs. 1C and 2B).
156 Numbers of cortical FjB positive cells at the level of the caudal
157 hippocampus were smaller than at the medial level but were
158 significant in two of the three cortical regions examined (Fig. 2B).
159 No significant FjB staining was found in cortical regions in the
160 contralateral hemisphere of KA-injected mice (data not shown).

161 2.4. FjB staining in the amygdala and lateral septal nucleus

162 As expected, FjB-positive cells were present within the
163 ipsilateral amygdala at the level of injection site in both KA-
164 injected and control mice (Fig. 4B). Counts of FjB-positive cells
165 were significantly higher in KA-injected mice compared to
166 controls in the ipsilateral amygdala at levels corresponding to
167 rostral and medial hippocampus (Figs. 3A,B and 4B). No FjB-

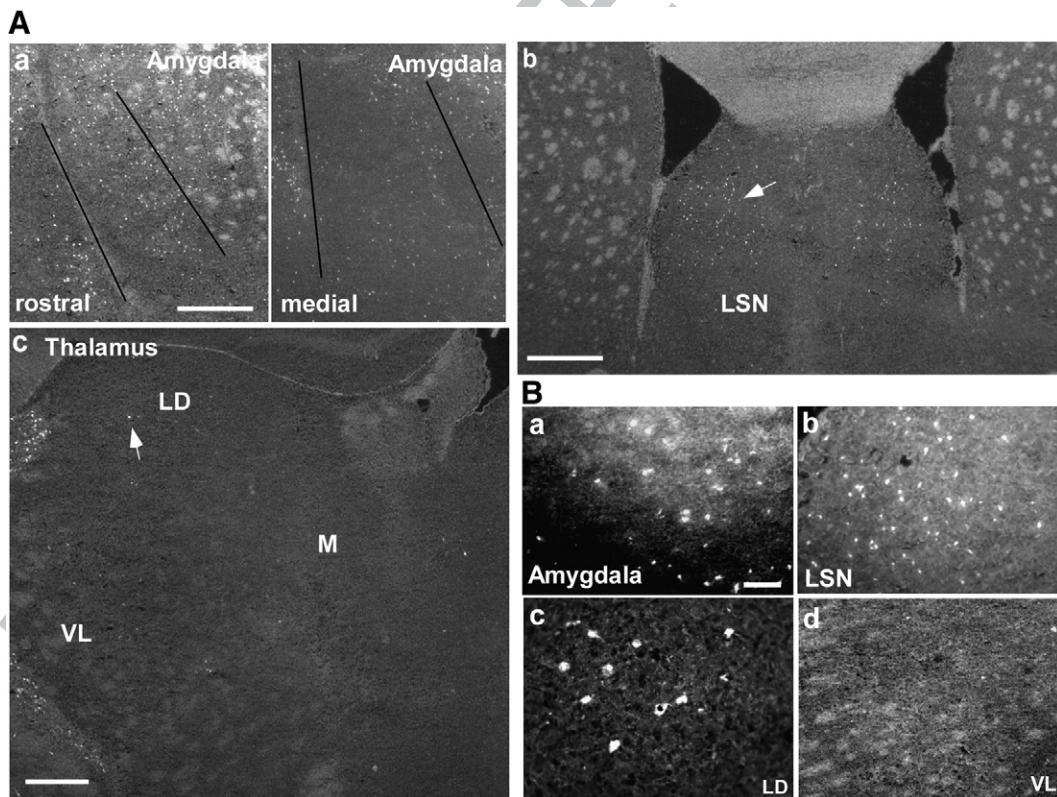


Fig. 3 – Seizure damage in amygdala, thalamus and lateral septal nucleus. (A) Representative photomicrographs from KA-treated mice at 24 h showing FjB staining within a, amygdala at rostral and medial levels, b lateral septal nucleus (LSN) and c thalamus. LD, lateral dorsal; VL, ventrolateral; M, medial. (B) Higher power (20× lens) images of FjB-stained cells in a, amygdala, b, lateral septal nucleus and c,d thalamic nuclei. Scale bars in A, 500 μm; B, 100 μm.

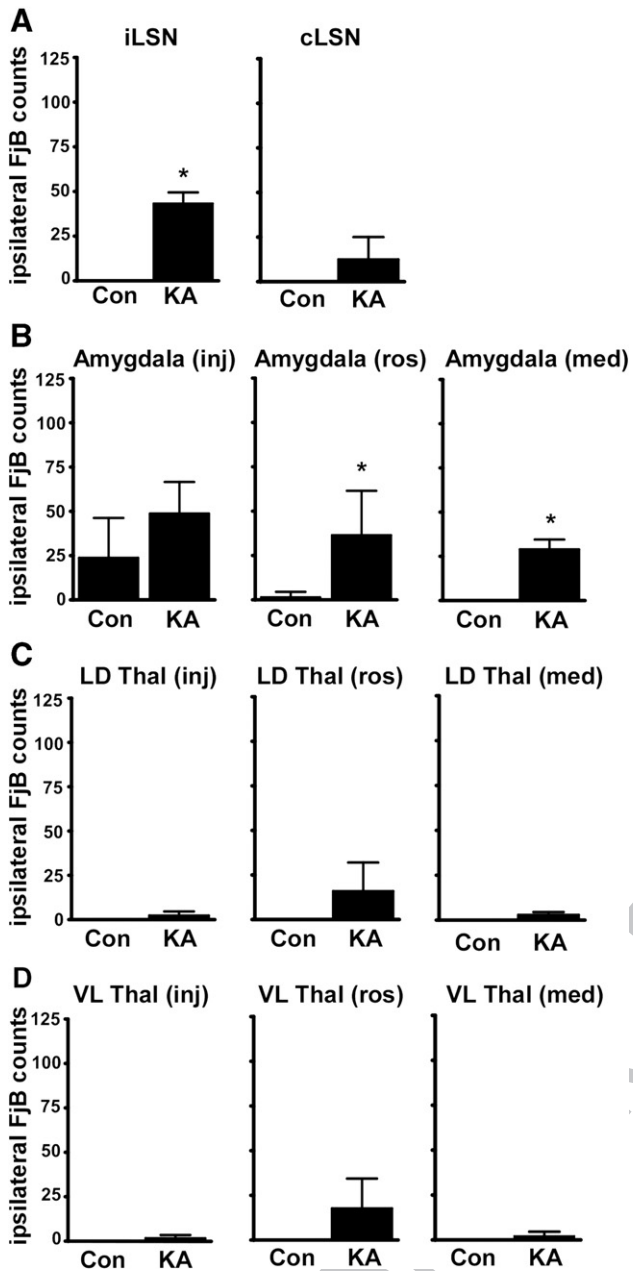


Fig. 4 – Quantification of seizure damage in lateral septal nucleus, amygdala and thalamus. (A) Counts of FjB-positive cells in control (Con) and seizure mice (KA) within the ipsilateral (i) and contralateral (c) lateral septal nucleus (LSN). **(B)** Counts of FjB-positive cells within the amygdala nucleus at the level of the injection (inj) point (AP, –0.96 mm), rostral (ros) and medial (med) levels. **(C)** Counts of FjB-positive cells in lateral dorsal (LD) and ventrolateral (VL) at the level of injection point, rostral hippocampus and medial hippocampus. Data are mean ± SD for n = 4 per group.

168 positive cells were present in the contralateral amygdala at
169 any level examined in control or KA-injected mice.

170 Significant FjB staining was detected in all KA-injected
171 mice within the ipsilateral lateral septal nucleus (LSN) at the
172 level of the amygdala injection point (Figs. 3A and 4A). FjB-

positive cells were present within the contralateral LSN in 50%
of KA-injected mice (Figs. 3A and 4A).

2.5. FjB staining in thalamus after seizures

Finally, we examined FjB staining at the level of the injection
point and rostral and medial hippocampus, for three thalamic
nuclei. Occasional scattered FjB-positive cells were present in
some KA-injected mice in the lateral–dorsal thalamus and
ventro-lateral thalamus at the level of rostral hippocampus
(Figs. 3A and 4C,D). Counts of thalamic FjB-positive cells showed
no significant difference between controls and KA-treated mice
and no FjB-positive cells were present in KA-injected mice on
the contralateral side for any of the thalamic areas at any level.

2.6. Short latency epileptogenesis following intra-amygdala KA microinjection in mice

The time of onset of spontaneous, recurrent seizures following
damage caused by intra-amygdala KA microinjection in mice
has not yet been investigated. To profile epileptogenesis in
this model we used implantable EEG telemetry units to record
surface EEG in freely-moving mice. Four mice were subject to
two weeks of 24 h/day EEG recordings after KA microinjection.
Intermittent EEG recordings from vehicle-injected mice did
not detect any epileptic seizures (data not shown).

No mice died after intra-amygdala KA microinjection or
during long-term recordings, and all mice developed sponta-
neous seizures (Fig. 5). Epileptic seizures were typically char-
acterized by a brief period of immobility during onset. This was
followed by jaw and forelimb clonus and elevated tail (Straub-
tail). Epileptic seizures typically progressed to rearing and falling
and in more severe events included loss of posture and jumping
(up to Racine scale 6).

The first day in which a spontaneous seizure was detected
by surface EEG was day 3 after KA microinjection (1 of 4 mice).
By day 4 after KA three of four mice had had an epileptic
seizure, and all mice had displayed an epileptic seizure by day
5 after KA microinjection (Fig. 5B). From day 4 thereafter, mice
averaged 1–4 seizures per day (full range 0–10). The average
electrographic seizure duration was 20.2 ± 15.1 s (range 10–90 s,
from 142 captured events). Daily spontaneous seizure rates
averaged across the group remained relatively consistent over
the course of the recording period (Fig. 5B). Spontaneous
seizures for individual mice showed variability between days
and across the recording period (Fig. 5C).

2.7. Hippocampal astrogliosis and mossy fiber rearrangement in epileptic mice

Finally, we examined sections from control mice and epileptic
mice killed on day 15 after the two week EEG recordings post-
KA, to visualize long-term changes to the hippocampus. NeuN
immunostaining confirmed the presence of macroscopic ipsi-
lateral CA3 lesions in epileptic mice (Fig. 6A). These were not
present on the contralateral side of epileptic mice (Fig. 6A).

Next, we counter-stained NeuN-labeled sections with anti-
bodies against glial fibrillary acidic protein (GFAP) as a marker of
astrogliosis. Examination of GFAP-stained hippocampi in epi-
leptic mice revealed increased staining in the ipsilateral CA3

227 region of epileptic mice, and the presence of thickened astrocyte
228 processes (Fig. 6B).

229 We also stained sections from epileptic mice for FjB to exam-
230 ine ongoing degenerative changes (Fig. 6C). Hippocampal FjB
231 staining was largely negative, although one epileptic mouse had
232 a small cluster of FjB-positive cells within ipsilateral CA3 (data

not shown) (Fig. 6C). A small number of FjB-positive cells (range
233 7–58) were also present in ipsilateral cortex in sections from
234 epileptic mice (data not shown). 235

Last, we undertook immunostaining for neuropeptide Y
236 (NPY) on hippocampal sections from epileptic mice, as a surro-
237 gate marker of mossy fiber axon rearrangement (Borges et al., 238
2003). Compared to control, there were prominent increases in
239 NPY immunoreactivity in ipsilateral hippocampus, including
240 mossy fibers throughout the suprapyramidal region of CA3 and
241 inner molecular layer of the dentate gyrus (Fig. 6D). While
242 asymmetric, increased NPY immunostaining in the mossy fiber
243 pathway was also apparent in the contralateral hippocampus
244 (Fig. 6D). 245

3. Discussion

In vivo models of prolonged seizures have been valuable tools for
246 advancing our understanding of the cell and molecular patho-
247 genesis of human MTLE (Morimoto et al., 2004). A majority of
248 hippocampi obtained from patients with temporal lobe epilepsy
249 display neuropathologic changes that comprise preferential
250 unilateral neuron loss within the endfolium and CA1, with rela-
251 tive sparing of CA2. Additional features include (astro)gliosis,
252 dentate granule cell layer dispersion and mossy fibre rearrange-
253 ment (Najm et al., 2006). Limitations exist with some animal
254 models in terms of reflecting this pathology. Systemic admin-
255 istration of pilocarpine or KA produces bilateral damage that is
256 often extensive in the cortex, while hippocampal damage, where
257 present, may be the result of secondary processes such as
258 ischemic hemorrhage (Fariello et al., 1989; Sloviter, 2005; Sloviter
259 et al., 2007). Commonly used mouse strains also lack character-
260 istic seizure damage in hippocampus after systemically-deliv-
261 ered convulsants (Schauwecker and Steward, 1997). Focal
262 elicitation approaches such as electrical stimulation of the per-
263 forant path appear to more faithfully model the unilateral and
264 hippocampal-predominant neuropathology of human MTLE
265 (Harvey and Sloviter, 2005; Kienzler et al., 2006; Sloviter, 1983;
266 Sloviter et al., 2007). An alternative approach has been to elicit
267 seizures by intra-amygdala KA microinjection. Originally des-
268 cribed in rats (Ben-Ari et al., 1980), we adapted this model to mice
269 (Araki et al., 2002; Shinoda et al., 2004a). While independent
270 groups have subsequently employed the model in mice (Kasugai
271 et al., 2007; Li et al., 2008), the present study provides important
272 additional characterization. First, our experiments show
273 damage in CA3 spans the full rostro-caudal extent of the ipsi-
274 lateral hippocampus and was similar at each level examined. 275
276
277

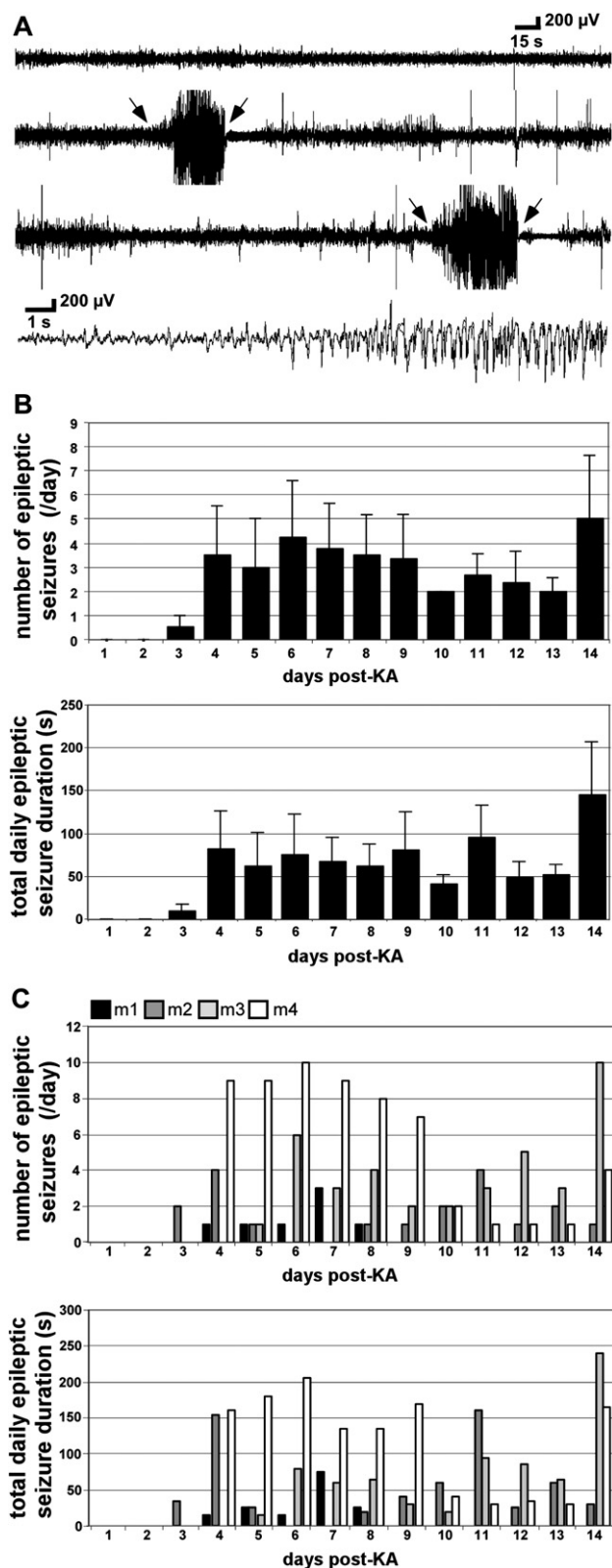


Fig. 5 – Temporal course of epilepsy emergence after intra-amygdala KA microinjection using radiotelemetry EEG in mice. (A) Representative EEG traces showing baseline EEG and examples of typical epileptic seizures captured by EEG telemetry (between arrows). Bottom trace shows typical electrographic seizure onset. (B) Graphs represent (top) average number of epileptic seizures per day, and (bottom) cumulative average duration of epileptic seizures per day. Data are mean \pm SD for $n=4$ per group. (C) Graphs showing daily seizure number and cumulative seizure time for the individual recorded mice (m).

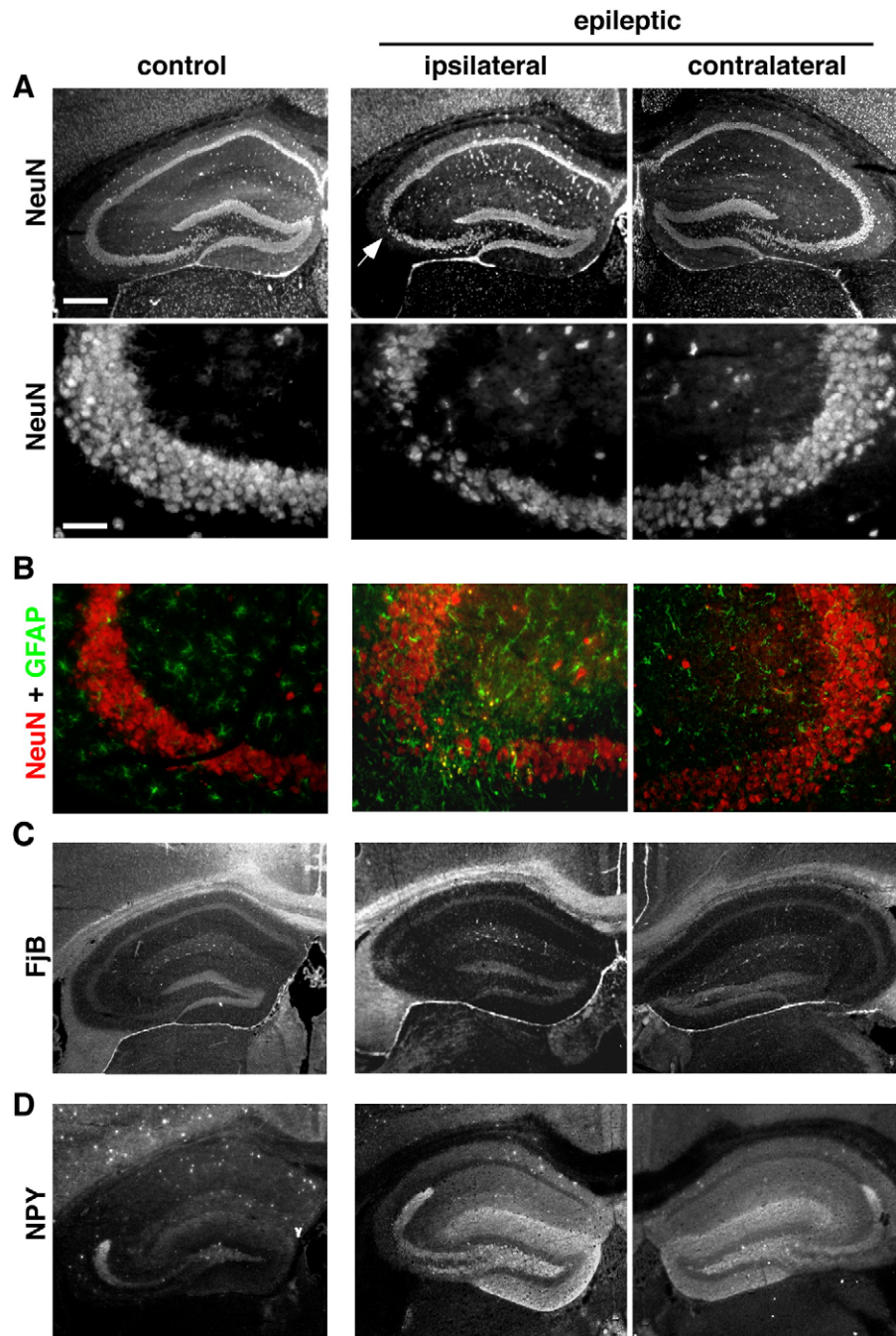


Fig. 6 – Chronic hippocampal changes in epileptic mice. Representative photomicrographs of hippocampal changes in the ipsilateral and contralateral hippocampi of epileptic mice. (A) Photomicrographs showing (top) 4× and (bottom) 20× lens field views of NeuN immunostaining in hippocampi from control and epileptic mice at day 15. Note the presence of a lesion in ipsilateral but not contralateral CA3 of epileptic mice (arrow). (B) Representative NeuN/GFAP double immunostaining (20× lens) in control and epileptic mice. Note elevated GFAP staining within the lesioned region of the ipsilateral CA3. (C,D) Representative photomicrographs (4× lens) showing FjB and neuropeptide Y (NPY) in control and epileptic mice. Note enhanced NPY staining in epileptic mice but lack of FjB staining. Scale bar in top left panel in A, C 500 μm; bottom left in A, 100 μm.

278 This supports the injury as seizure-related, rather than a result
 279 of diffusion of KA from the injection site. Indeed, the extent of
 280 the CA3 lesion can be further restricted by administering
 281 lorazepam 30 min after intra-amygdala KA microinjection in
 282 this model (Li et al., 2008). The CA2 subfield was not damaged by
 283 intra-amygdala KA-induced seizures, in agreement with the

resistance reported previously using this model (Araki et al., 284
 2002; Kasugai et al., 2007; Li et al., 2008; Shinoda et al., 2004a). 285
 Damage to CA1 is often present in human MTLE and we find as 286
 before (Araki et al., 2002; Shinoda et al., 2004a), that CA1 injury, 287
 though not strongly induced, is nonetheless present in mice 288
 after intra-amygdala KA microinjection, particularly in temporal 289

hippocampus. Since human MTLE pathology is mainly unilateral and affects the hilar, CA3 and CA1 hippocampal subfields, the present study supports the relevance of the modeling approach and species used.

Cortical neuronal injury has not previously been investigated following intra-amygdala KA microinjection in mice. The present study shows only small numbers of ipsilateral cortical neurons are damaged in this model. This matches similar findings in rats with this model (Henshall et al., 2002), and supports the clinical relevance of the model since cortical neuron loss in human MTLE is typically limited or absent (Bothwell et al., 2001; Dawodu and Thom, 2005; Doherty et al., 2003). The model does not appear to evoke significant damage to the thalamus, which is an area vulnerable in some models (Kubova et al., 2001) and in patients after status epilepticus (Fujikawa et al., 2000). Experimental SE often causes amygdala injury (Nissinen et al., 2000; Tuunanen et al., 1999), and this was seen in the present study, although injury at the rostral extent likely resulted from mechanical (cannula) or direct excitotoxic effects of KA. A limitation of the model lies with achieving complete seizure cessation after intra-amygdala KA microinjection. However, some control is possible through varying anticonvulsant administration time (Araki et al., 2002; Li et al., 2008; Shinoda et al., 2004a). An additional advantage of the present model is its adaptability for use in genetically-modified mice, where it has recently been employed to characterize the anti-apoptotic role of *bcl-w* (Murphy et al., 2007) and epileptogenic effects of adenosine kinase (Li et al., 2008).

A latent period between an initial precipitating neurological injury and subsequent emergence of epileptic seizures is characteristic of acquired MTLE (Williams et al., 2007). Latent periods of a month or more are typically reported for experimental SE-induced epilepsy (Morimoto et al., 2004; Pitkanen et al., 2007). However, spontaneous seizure onset has been detected in subgroups of animals within a week of SE using both systemic and focal elicitation approaches (Harvey and Sloviter, 2005; Nissinen et al., 2000; Shibley and Smith, 2002). By undertaking continuous EEG recordings we could detect epileptic seizures within 3–4 days of intra-amygdala KA-induced SE, with all tested mice epileptic by day 5. This short latent period may result from the localized, reproducible damage in this model and the fidelity of continuous EEG monitoring post-KA (Williams et al., 2007). Our data are consistent with awareness that apparently protracted latent periods in some animals or in some models result in part from inter-animal variability, the extent of hippocampal injury after SE or intermittent EEG monitoring (Williams et al., 2007). The short latent period here also implies protracted pathological processes are unlikely responsible for the emergence of spontaneous seizures in the present model. Mossy fiber sprouting has been linked to the formation of epileptic circuits (Dudek et al., 1994; Wuarin and Dudek, 1996) and can precede emergence of spontaneous seizures (Hendriksen et al., 2001). However, spontaneous seizures occur in post-SE animals without mossy fiber sprouting and the frequency of epileptic events may bear little relation to the extent of sprouting (Nissinen et al., 2000, 2001; Williams et al., 2002). While not excluding a role, the early onset of spontaneous seizures in the present model probably undermines a significant contribution. Nevertheless, mossy fiber sprouting,

as implied by NPY immunostaining, was apparent in (epileptic) mice 15 days after KA. The present study also identified astrogliosis within the field of primary damage within the hippocampus. This supports work by Li et al. using the same model, which implicated overexpression of adenosine kinase secondary to astrogliosis in CA3 in epileptic seizure generation (Li et al., 2008).

Neuropeptide Y is an endogenous modulator of excitability and potent inhibitor of seizures. Our data show its presence in normal hippocampus and elevation in hippocampus of epileptic mice, in accordance with reports in chronically epileptic rodents (Nissinen et al., 2000; Schwarzer et al., 1995; Vezzani et al., 1994) and studies showing its elevation in the terminals of mossy fibres (Tu et al., 2005; Vezzani et al., 1996). Whether increased hippocampal NPY levels influences epileptic seizures in the present model is unknown, but anticonvulsant and seizure-terminating roles are supported by findings in mice deficient in NPY which display spontaneous seizures and have increased sensitivity to kainic acid, effects reversed by intracerebral NPY administration (Baraban et al., 1997). Transgenic or viral vector-mediated NPY overexpression in rats also reduces seizures, seizure susceptibility and epileptogenesis (Richichi et al., 2004; Vezzani et al., 2002; Woldbye et al., 1997). However, some data are consistent with seizure-promoting actions of NPY (Liu et al., 1999; Vezzani et al., 1994).

The percentage of animals developing epilepsy after SE shows variance according to model and monitoring employed (Williams et al., 2007). High rates (~90%) are reported following electrical amygdala-stimulation (Nissinen et al., 2000; Pitkanen et al., 2005) and all C57Bl/6 mice surviving pilocarpine-induced SE become epileptic (Borges et al., 2003; Shibley and Smith, 2002). In agreement with findings from hippocampal EEG recordings in mice three weeks after intra-amygdala KA microinjection (Li et al., 2008), we found all mice in our study became epileptic. This supports high-reproducibility of epileptogenesis in this model. However, variability in outcome may be a desired characteristic, for instance for identification of surrogate or biomarkers among animals subject to the same initial precipitating injury.

Daily epileptic event rates remain quite constant in models of amygdala-triggered SE (Nissinen et al., 2000), although the proportion of partial versus secondarily generalized seizures may change (Nissinen et al., 2000; Tanaka et al., 1988). Inter-animal differences in daily event number were found in the present model, but when averaged across the group the daily seizure frequency remained quite consistent once epilepsy emerged. Epileptic seizure durations found in our model were on average of shorter duration than those reported after electrical stimulation of the amygdala (Nissinen et al., 2000; Pitkanen et al., 2007). Since damage was bi-lateral in the studies of Nissinen et al., this supports the influence of the extent of damage and regions affected in the epileptic phenotype.

A relationship between the duration or intensity of SE as the initial precipitating injury and subsequent epileptic phenotype has been demonstrated (Klitgaard et al., 2002; Nissinen et al., 2000; Pitkanen et al., 2005). Moreover, a critical threshold of hilar interneuron loss may be the minimal substrate for formation of epileptic circuits (Zappone and Sloviter, 2004). Taken together, our data are consistent with relatively restricted and unilateral hippocampal neuronal death being sufficient for epileptogenesis. 409

410 Interestingly, mice subject to intra-amygdala KA microinjection
411 that have a lesion restricted to ipsilateral CA3a display
412 hippocampal-only seizures (Li et al., 2008). Monitoring in that
413 study was only during a single day three weeks post-KA and so
414 may have missed some secondarily generalized events. Never-
415 theless, these data suggest damage in addition to CA3a under-
416 lies the expression of seizures we detected on surface EEG.
417 Preventing neuronal death by primary (e.g. glutamate antago-
418 nists) or secondary (downstream cell death signaling pathways)
419 neuroprotective agents may therefore be critical to blocking or
420 mitigating epilepsy after SE (Meldrum, 2002). However, results
421 from some studies challenge the efficacy of either class of
422 neuroprotectant as an approach to anti-epileptogenesis (Brandt
423 et al., 2003; Narkilahti et al., 2003).

424 In conclusion, the present study provides a more complete
425 characterization of the acute hippocampal and extra-hippo-
426 campal damage incurred by seizures after intra-amygdala KA
427 microinjection in mice. The pattern of damage reflects that
428 common to human MTLE and the injury elicits epilepsy within a
429 short latent period. Accordingly, intra-amygdala KA microinjec-
430 tion in mice may provide a suitable means for modeling the
431 pathogenesis of MTLE and studying its genetic architecture.

4. Experimental procedures

4.1. Seizure model

435 Animal experiments were carried out in accordance with the
436 principals of the European Communities Council Directive (86/
437 609/EEC) and National Institute of Health's *Guide for the Care and*
438 *Use of Laboratory Animals*. Procedures were reviewed and approved
439 by the Research Ethics Committee of the Royal College of Sur-
440 geons in Ireland, under license from the Department of Health,
441 Dublin, Ireland.

442 Studies were performed according to previously described
443 techniques (Murphy et al., 2007; Shinoda et al., 2004a). Mice
444 (C57BL/6 adult male, 20–25 g) were obtained from Harlan, UK. Mice
445 were anesthetized using isoflurane (3–5%) and maintained nor-
446 mothemic by means of a feedback-controlled heat blanket
447 (Harvard Apparatus Ltd, Kent, England). A catheter was inserted
448 into the femoral vein for administration of anticonvulsant. Mice
449 were next placed in a stereotaxic frame and following a midline
450 scalp incision three partial craniectomies were performed and
451 mice were affixed with cortical electrodes (Bilaney Consultants
452 Ltd, Sevenoaks, UK) to record surface EEG. Electrodes were placed
453 above dorsal hippocampus and a third over frontal cortex. EEG
454 was recorded using a Grass Comet digital EEG (Medivent Ltd,
455 Lucan, Ireland). A guide cannula was affixed (coordinates from
456 Bregma: AP = -0.94; L = -2.85 mm) (Franklin and Paxinos, 1997)
457 and the entire skull assembly fixed in place with dental cement.
458 Anesthesia was then discontinued and freely moving mice were
459 placed in a clear Perspex recording chamber. EEG recordings were
460 commenced and after establishing baseline EEG for a few minutes
461 mice were lightly restrained by the experimenter to permit low-
462 ering of an injection cannula through the guide cannula to 3.75 mm
463 below the dura for microinjection of KA (Ocean Produce Interna-
464 tional, Nova Scotia, Canada) (0.3 µg in 0.2 µl phosphate-buffered
465 saline, PBS) into the basolateral amygdala nucleus. Non-seizure
466 control mice received the same volume of intra-amygdala vehicle.

467 Forty minutes following microinjection of KA or vehicle, mice
468 received intravenous lorazepam (6 mg/kg) and the EEG monitored
469 for up to 1 h thereafter. Administration of lorazepam was used to
470 curtail status epilepticus, thereby reducing mortality, morbidity
471 and restricting the extent of damage, as described previously
472 (Shinoda et al., 2004a). Mice were euthanized 24 h following lora-
473 zepam and perfused with saline to remove intravascular blood
474 components. Brains were flash-frozen whole in 2-methylbutane
475 at -30 °C and processed for histopathology as described below.

4.2. Analysis of spontaneous seizures using EEG telemetry

477 A separate group of mice were subject to long-term EEG
478 monitoring to detect the emergence of spontaneous seizures.
479 For these purposes, EEG was recorded using implantable EEG
480 telemetry units (Data Systems International, St. Paul, MN) ac-
481 cording to previously reported techniques with modifications
482 (Weiergraber et al., 2005). EEG data were acquired using the
483 Dataquest A.R.T. system with EEG transmitters (Model: F20-
484 EET, DSI) configured to record 2 channel EEG that were affixed
485 over dorsal hippocampi/temporal cortex under anesthesia.
486 Transmitter units were placed in a subcutaneous pocket along
487 the dorsal flank. Following surgery and KA-induced seizures,
488 units were activated and telemetry recordings commenced for
489 14 days from cages on top of receivers (RPC-1), thus allowing
490 free movement and access to food and water. Continuous EEG
491 data was transferred to a PC via a Data Exchange Matrix (DSI).
492 Mice were euthanized on day 15 and brains processed for
493 histopathology and immunostaining as described above. Tele-
494 metry EEG recordings were manually analyzed with epileptic
495 seizures defined according to Pitkanen et al. (Pitkanen et al.,
496 2005) as high frequency (>5 Hz) high amplitude (>2 baseline)
497 polyspike discharges of ≥5 s duration.

4.3. Behaviour

498 Mice were observed during KA-induced seizures and also during
499 spontaneous epileptic seizures and scored according to a modi-
500 fied Racine scale for mice (Borges et al., 2003). Score 0, normal
501 activity; Score 1, arrest and rigid posture or immobility; Score 2,
502 stiffened or extended tail; Score 3, partial body clonus, including
503 forelimb clonus or head bobbing; Score 4, rearing; Score 5, rea-
504 ring and falling; Score 6 tonic-clonic seizures with loss of pos-
505 ture or jumping.

4.4. Histopathology

506 Brains were sectioned at 12 µm on a Leica cryostat at four
507 stereotaxic levels (AP from Bregma; -0.94 mm (injection point),
508 -1.22 mm (rostral hippocampus), -1.82 mm (medial hippo-
509 campus) and -2.92 mm (caudal hippocampus)) according to a
510 mouse stereotaxic atlas (Franklin and Paxinos, 1997). Brain
511 regions studied were ipsilateral and contralateral to injection
512 side as follows: lateral septal nucleus, basolateral amygdala,
513 hippocampal hilus, CA3 and CA1, temporal cortex, entorhinal
514 cortex, perirhinal cortex, piriform cortex, lateral-dorsal thala-
515 mus, medio-dorsal thalamus and ventro-lateral thalamus.

516 Neuronal damage was assessed using the FluoroJade B (FJB)
517 technique. Briefly, sections were air-dried and post-fixed in 10%
518 formalin. Next, sections were immersed in 100% ethanol (3 min),
519

521 followed by immersion in 70% ethanol (1 min) then rinsed in
522 distilled water (1 min). Sections were next transferred to fresh
523 0.006% potassium permanganate solution for 15 min with gentle
524 shaking. Sections were then rinsed again and transferred to FJB
525 solution (0.001% in 0.1% acetic acid) (Chemicon Europe Ltd,
526 Chandlers Ford, UK). After staining, sections were rinsed again,
527 dried, cleared and mounted in DPX (Sigma-Aldrich). Sections
528 were examined using a Nikon 2000s epifluorescence microscope
529 (Micro-optica, Dublin, Ireland) under Ex/Em wavelengths of 330–
530 380/420 nm (blue), 472/520 nm (green) and 540–580/600–660 nm
531 (red) and imaged using a Hamamatsu Orca 285 camera. Pseudo-
532 colour transforms from monochromatic Hamamatsu Orca 285
533 images were undertaken using Adobe® Photoshop® 6.0. FJB
534 positive cells were the average of two adjacent sections counted
535 by an observer blinded to experimental treatment (Shinoda
536 et al., 2004a,b).

537 4.5. Immunohistochemistry

538 Immunohistochemistry was undertaken according to previously
539 described techniques (Murphy et al., 2007). Briefly, fresh-frozen
540 sections (12 µm) were air-dried, post-fixed in 10% formalin and
541 washed in PBS. Next, sections were permeabilized with 0.3%
542 Triton X-100 and blocked in 5% goat serum for 1 h. Sections were
543 then incubated overnight with antibodies against NeuN (Chem-
544 icon) or GFAP (Sigma-Aldrich) (both 1:500), or neuropeptide Y
545 (NPY, 1:1000) (Sigma-Aldrich), were washed again in PBS and
546 incubated in goat anti-mouse AlexaFluor 568 (for NeuN and
547 GFAP) and goat anti-rabbit AlexaFluor 488 (for NPY) (Bio Sciences
548 Ltd, Dun Laoghaire, Ireland). Sections were mounted with me-
549 dium containing 4',6 diamidino-2-phenylindole (DAPI) (Vector
550 Laboratories Ltd, Peterborough, UK) to visualize nuclei and
551 fluorescence immunostaining examined as described above.

552 4.6. Statistical analysis

553 Data are presented as mean ± SD. Comparison of data was
554 performed using a Mann–Whitney *U* test and significance was
555 accepted at $p < 0.05$.

556 Acknowledgments

558 This research was supported by Science Foundation Ireland
559 grant IN3/04/B466, HRB grants EQ/2004/32 and RP/2005/24 and
560 by Wellcome Trust grant GR076576MA. The authors would like
561 to thank Ina Woods for technical support and Jochen Prehn for
562 helpful advice on the manuscript.

563 REFERENCES

565 Araki, T., Simon, R.P., Taki, W., Lan, J.-Q., Henshall, D.C., 2002.
566 Characterization of neuronal death induced by focally evoked
567 limbic seizures in the C57BL/6 mouse. *J. Neurosci. Res.* 69,
568 614–621.
569 Baraban, S.C., Hollopeter, G., Erickson, J.C., Schwartzkroin, P.A.,
570 Palmiter, R.D., 1997. Knock-out mice reveal a critical antiepileptic
571 role for neuropeptide Y. *J. Neurosci.* 17, 8927–8936.
572 Ben-Ari, Y., Tremblay, E., Ottersen, O.P., 1980. Injections of kainic
573 acid into the amygdaloid complex of the rat: an electrographic,

clinical and histological study in relation to the pathology of 574
epilepsy. *Neuroscience* 5, 515–528. 575
Borges, K., Gearing, M., McDermott, D.L., Smith, A.B., Almonte, A.G., 576
Wainer, B.H., Dingledine, R., 2003. Neuronal and glial pathological 577
changes during epileptogenesis in the mouse pilocarpine model. 578
Exp. Neurol. 182, 21–34. 579
Bothwell, S., Meredith, G.E., Phillips, J., Staunton, H., Doherty, C., 580
Grigorenko, E., Glazier, S., Deadwyler, S.A., O'Donovan, C.A., 581
Farrell, M., 2001. Neuronal hypertrophy in the neocortex 582
of patients with temporal lobe epilepsy. *J. Neurosci.* 21, 583
4789–4800. 584
Brandt, C., Potschka, H., Loscher, W., Ebert, U., 2003. 585
N-methyl-D-aspartate receptor blockade after status epilepticus 586
protects against limbic brain damage but not against epilepsy in 587
kainate model of temporal lobe epilepsy. *Neuroscience* 118, 588
727–740. 589
Chang, B.S., Lowenstein, D.H., 2003. *Epilepsy. N. Engl. J. Med.* 349, 590
1257–1266. 591
Dawodu, S., Thom, M., 2005. Quantitative neuropathology of the 592
entorhinal cortex region in patients with hippocampal sclerosis 593
and temporal lobe epilepsy. *Epilepsia* 46, 23–30. 594
DeGiorgio, C.M., Tomiyasu, U., Gott, P.S., Treiman, D.M., 1992. 595
Hippocampal pyramidal cell loss in human status epilepticus. 596
Epilepsia 33, 23–27. 597
Doherty, C.P., Fitzsimons, M., Meredith, G., Thornton, J., McMackin, 598
D., Farrell, M., Phillips, J., Staunton, H., 2003. Rapid stereological 599
quantitation of temporal neocortex in TLE. *Magn. Reson.* 600
Imaging 21, 511–518. 601
Du, F., Whetsell Jr., W.O., Abou-Khalil, B., Blumenkopf, B., Lothman, 602
E.W., Schwarcz, R., 1993. Preferential neuronal loss in layer III of 603
the entorhinal cortex in patients with temporal lobe epilepsy. 604
Epilepsy Res. 16, 223–233. 605
Dudek, F.E., Obenaus, A., Schweitzer, J.S., Wuarin, J.P., 1994. 606
Functional significance of hippocampal plasticity in epileptic 607
brain: electrophysiological changes of the dentate granule cells 608
associated with mossy fiber sprouting. *Hippocampus* 4, 609
259–265. 610
Engel Jr., J., 2001. Mesial temporal lobe epilepsy: what have we 611
learned? *Neuroscientist* 7, 340–352. 612
Fariello, R.G., Golden, G.T., Smith, G.G., Reyes, P.F., 1989. Potentiation 613
of kainic acid epileptogenicity and sparing from neuronal damage 614
by an NMDA receptor antagonist. *Epilepsy Res.* 3, 206–213. 615
Franklin, K.B.J., Paxinos, P., 1997. *The mouse brain in stereotaxic* 616
coordinates. Academic Press, Inc, San Diego. 617
Fujikawa, D.G., Itabashi, H.H., Wu, A., Shinmei, S.S., 2000. Status 618
epilepticus-induced neuronal loss in humans without systemic 619
complications or epilepsy. *Epilepsia* 41, 981–991. 620
Gouder, N., Fritschy, J.M., Boison, D., 2003. Seizure suppression by 621
adenosine A1 receptor activation in a mouse model of 622
pharmacoresistant epilepsy. *Epilepsia* 44, 877–885. 623
Harvey, B.D., Sloviter, R.S., 2005. Hippocampal granule cell activity 624
and c-Fos expression during spontaneous seizures in awake, 625
chronically epileptic, pilocarpine-treated rats: implications for 626
hippocampal epileptogenesis. *J. Comp. Neurol.* 488, 442–463. 627
Hendriksen, H., Datson, N.A., Ghijsen, W.E., van Vliet, E.A., da 628
Silva, F.H., Gorter, J.A., Vreugdenhil, E., 2001. Altered hippocampal 629
gene expression prior to the onset of spontaneous seizures in the 630
rat post-status epilepticus model. *Eur. J. Neurosci.* 14, 1475–1484. 631
Henshall, D.C., Araki, T., Schindler, C.K., Lan, J.-Q., Tiekoter, K., 632
Taki, W., Simon, R.P., 2002a. Activation of Bcl-2-associated 633
death protein and counter-response of Akt within cell populations 634
during seizure-induced neuronal death. *J. Neurosci.* 22, 8458–8465. 635
Henshall, D.C., Sinclair, J., Simon, R.P., 2000b. Spatio-temporal 636
profile of DNA fragmentation and its relationship to patterns of 637
epileptiform activity following focally evoked limbic seizures. 638
Brain Res. 858, 290–302. 639
Hudson, L.P., Munoz, D.G., Miller, L., McLachlan, R.S., Girvin, J.P., 640
Blume, W.T., 1993. Amygdaloid sclerosis in temporal lobe 641
epilepsy. *Ann. Neurol.* 33, 622–631. 642

- 643 Kasugai, M., Akaike, K., Imamura, S., Matsukubo, H., Tojo, H.,
644 Nakamura, M., Tanaka, S., Sano, A., 2007. Differences in two
645 mice strains on kainic acid-induced amygdalar seizures.
646 *Biochem. Biophys. Res. Commun.* 357, 1078–1083.
- 647 Kienzler, F., Jedlicka, P., Vuksic, M., Deller, T., Schwarzacher, S.W.,
648 2006. Excitotoxic hippocampal neuron loss following sustained
649 electrical stimulation of the perforant pathway in the mouse.
650 *Brain Res.* 1085, 195–198.
- 651 Klitgaard, H., Matagne, A., Vanneste-Goemaere, J., Margineanu, D.G.,
652 2002. Pilocarpine-induced epileptogenesis in the rat: impact of
653 initial duration of status epilepticus on electrophysiological and
654 neuropathological alterations. *Epilepsy Res.* 51, 93–107.
- 655 Kubova, H., Druga, R., Lukasiuk, K., Suchomelova, L., Haugvicova, R.,
656 Jirmanova, I., Pitkanen, A., 2001. Status epilepticus causes
657 necrotic damage in the mediodorsal nucleus of the thalamus in
658 immature rats. *J. Neurosci.* 21, 3593–3599.
- 659 Li, T., Ren, G., Lusardi, T., Wilz, A., Lan, J.Q., Iwasato, T., Itoharu, S.,
660 Simon, R.P., Boison, D., 2008. Adenosine kinase is a target for
661 the prediction and prevention of epileptogenesis in mice.
662 *J. Clin. Invest.* 118, 571–582.
- 663 Liu, H., Mazarati, A.M., Katsumori, H., Sankar, R., Wasterlain, C.G.,
664 1999. Substance P is expressed in hippocampal principal
665 neurons during status epilepticus and plays a critical role
666 in the maintenance of status epilepticus. *Proc. Natl. Acad. Sci.*
667 *U. S. A.* 96, 5286–5291.
- 668 Mathern, G.W., Babb, T.L., Armstrong, D.L., 1997. Hippocampal
669 Sclerosis. In: Engel, J.J., Pedley, T.A. (Eds.), *Epilepsy: a*
670 *comprehensive textbook*, Vol. 13. Lippincott-Raven Publishers,
671 Philadelphia, pp. 133–155.
- 672 Meldrum, B.S., 2002. Implications for neuroprotective treatments.
673 *Prog. Brain Res.* 135, 487–495.
- 674 Meldrum, B.S., Bruton, C.J., 1992. *Epilepsy*. In: Adams, J.H., Duchen,
675 L.W. (Eds.), *Greenfield's Neuropathology*, Vol. 19. Oxford
676 University Press, New York, pp. 1246–1283.
- 677 Menini, C., Meldrum, B.S., Riche, D., Silva-Comte, C., Stutzmann, J.M.,
678 1980. Sustained limbic seizures induced by intraamygdaloid
679 kainic acid in the baboon: symptomatology and
680 neuropathological consequences. *Ann. Neurol.* 8, 501–509.
- 681 Morimoto, K., Fahnestock, M., Racine, R.J., 2004. Kindling and
682 status epilepticus models of epilepsy: rewiring the brain. *Prog.*
683 *Neurobiol.* 73, 1–60.
- 684 Murphy, B., Dunleavy, M., Shinoda, S., Schindler, C., Meller, R.,
685 Bellver-Estelles, C., Hatazaki, S., Dicker, P., Yamamoto, A.,
686 Koegel, I., Chu, X., Wang, W., Xiong, Z., Prehn, J., Simon, R.,
687 Henshall, D., 2007. Bcl-w protects hippocampus during
688 experimental status epilepticus. *Am. J. Pathol.* 171, 1258–1268.
- 689 Najm, I., Duvernoy, H., Schuele, S., 2006. Hippocampal anatomy
690 and hippocampal sclerosis. In: Wyllie, E. (Ed.), *The treatment*
691 *of epilepsy*. Lippincott Williams & Wilkins, Philadelphia,
692 pp. 55–68.
- 693 Narkilahti, S., Nissinen, J., Pitkanen, A., 2003. Administration of
694 caspase 3 inhibitor during and after status epilepticus in rat:
695 effect on neuronal damage and epileptogenesis.
696 *Neuropharmacology* 44, 1068–1088.
- 697 Nissinen, J., Halonen, T., Koivisto, E., Pitkanen, A., 2000. A new
698 model of chronic temporal lobe epilepsy induced by electrical
699 stimulation of the amygdala in rat. *Epilepsy Res.* 38, 177–205.
- 700 Nissinen, J., Lukasiuk, K., Pitkanen, A., 2001. Is mossy fiber
701 sprouting present at the time of the first spontaneous seizures
702 in rat experimental temporal lobe epilepsy? *Hippocampus* 11,
703 299–310.
- 704 Parent, J.M., Yu, T.W., Leibowitz, R.T., Geschwind, D.H., Sloviter, R.S.,
705 Lowenstein, D.H., 1997. Dentate granule cell neurogenesis is
706 increased by seizures and contributes to aberrant network
707 reorganization in the adult rat hippocampus. *J. Neurosci.* 17,
708 3727–3738.
- 709 Pitkanen, A., Tuunainen, J., Kalviainen, R., Partanen, K., Salmenpera,
710 T., 1998. Amygdala damage in experimental and human
711 temporal lobe epilepsy. *Epilepsy Res.* 32, 233–253.
- Pitkanen, A., Kharatishvili, I., Narkilahti, S., Lukasiuk, K., Nissinen, J., 712
2005. Administration of diazepam during status epilepticus 713
reduces development and severity of epilepsy in rat. *Epilepsy* 714
Res. 63, 27–42. 715
- Pitkanen, A., Kharatishvili, I., Karhunen, H., Lukasiuk, K., Immonen, R., 716
Nairismagi, J., Grohn, O., Nissinen, J., 2007. Epileptogenesis in 717
experimental models. *Epilepsia* 48 (Suppl 2), 13–20. 718
- Richichi, C., Lin, E.J., Stefanin, D., Colella, D., Ravizza, T., 719
Grignaschi, G., Veglianese, P., Sperk, G., Doring, M.J., Vezzani, A., 720
2004. Anticonvulsant and antiepileptogenic effects mediated 721
by adeno-associated virus vector neuropeptide Y expression in 722
the rat hippocampus. *J. Neurosci.* 24, 3051–3059. 723
- Schauwecker, P.E., Steward, O., 1997. Genetic determinants of 724
susceptibility to excitotoxic cell death: implications for gene 725
targeting approaches. *Proc. Natl. Acad. Sci. U. S. A.* 94,
726 4103–4108. 727
- Schwarzer, C., Williamson, J.M., Lothman, E.W., Vezzani, A., Sperk, G., 728
1995. Somatostatin, neuropeptide Y, neurokinin B and 729
cholecystokinin immunoreactivity in two chronic models of 730
temporal lobe epilepsy. *Neuroscience* 69, 831–845. 731
- Shibley, H., Smith, B.N., 2002. Pilocarpine-induced status epilepticus 732
results in mossy fiber sprouting and spontaneous seizures in 733
C57BL/6 and CD-1 mice. *Epilepsy Res.* 49, 109–120. 734
- Shinoda, S., Araki, T., Lan, J.Q., Schindler, C.K., Simon, R.P., Taki, W., 735
Henshall, D.C., 2004a. Development of a model of 736
seizure-induced hippocampal injury with features of 737
programmed cell death in the BALB/c mouse. *J. Neurosci. Res.* 738
76, 121–128. 739
- Shinoda, S., Schindler, C.K., Meller, R., So, N.K., Araki, T., 740
Yamamoto, A., Lan, J.Q., Taki, W., Simon, R.P., Henshall, D.C., 741
2004b. Bim regulation may determine hippocampal 742
vulnerability after injurious seizures and in temporal lobe 743
epilepsy. *J. Clin. Invest.* 113, 1059–1068. 744
- Sloviter, R.S., 1983. "Epileptic" brain damage in rats induced by 745
sustained electrical stimulation of the perforant path. I. Acute 746
electrophysiological and light microscopic studies. *Brain Res.* 747
Bull. 10, 675–697. 748
- Sloviter, R.S., 2005. The neurobiology of temporal lobe epilepsy: too 749
much information, not enough knowledge. *C. R. Biol.* 328, 143–153. 750
- Sloviter, R.S., Zappone, C.A., Bumanglag, A.V., Norwood, B.A., 751
Kudrimoti, H., 2007. On the relevance of prolonged convulsive 752
status epilepticus in animals to the etiology and neurobiology 753
of human temporal lobe epilepsy. *Epilepsia* 48 (Suppl 8), 6–10. 754
- Tanaka, T., Kaijima, M., Yonemasu, Y., Cepeda, C., 1985. 755
Spontaneous secondarily generalized seizures induced by a 756
single microinjection of kainic acid into unilateral amygdala in 757
cats. *Electroencephalogr. Clin. Neurophysiol.* 61, 422–429. 758
- Tanaka, S., Kondo, S., Tanaka, T., Yonemasu, Y., 1988. Long-term 759
observation of rats after unilateral intra-amygdaloid injection 760
of kainic acid. *Brain Res.* 463, 163–167. 761
- Tu, B., Timofeeva, O., Jiao, Y., Nadler, J.V., 2005. Spontaneous 762
release of neuropeptide Y tonically inhibits recurrent mossy 763
fiber synaptic transmission in epileptic brain. *J. Neurosci.* 25,
764 1718–1729. 765
- Tuunainen, J., Lukasiuk, K., Halonen, T., Pitkanen, A., 1999. Status 766
epilepticus-induced neuronal damage in the rat amygdaloid 767
complex: distribution, time-course and mechanisms 768
Neuroscience 94, 473–495. 769
- Vezzani, A., Civenni, G., Rizzi, M., Monno, A., Messali, S., Samanin, R., 770
1994. Enhanced neuropeptide Y release in the hippocampus is 771
associated with chronic seizure susceptibility in kainic acid 772
treated rats. *Brain Res.* 660, 138–143. 773
- Vezzani, A., Schwarzzer, C., Lothman, E.W., Williamson, J., Sperk, G., 774
1996. Functional changes in somatostatin and neuropeptide Y 775
containing neurons in the rat hippocampus in chronic models 776
of limbic seizures. *Epilepsy Res.* 26, 267–279. 777
- Vezzani, A., Conti, M., De Luigi, A., Ravizza, T., Moneta, D., 778
Marchesi, F., De Simoni, M.G., 1999. Interleukin-1beta 779
immunoreactivity and microglia are enhanced in the rat 780

- 781 hippocampus by focal kainate application: functional evidence
782 for enhancement of electrographic seizures. *J. Neurosci.* 19,
783 5054–5065.
- 784 Vezzani, A., Michalkiewicz, M., Michalkiewicz, T., Moneta, D.,
785 Ravizza, T., Richichi, C., Aliprandi, M., Mule, F., Pirona, L., Gobbi, M.,
786 Schwarzer, C., Sperk, G., 2002. Seizure susceptibility and
787 epileptogenesis are decreased in transgenic rats overexpressing
788 neuropeptide Y. *Neuroscience* 110, 237–243.
- 789 Weiergraber, M., Henry, M., Hescheler, J., Smyth, N., Schneider, T.,
790 2005. Electrographic and deep intracerebral EEG
791 recording in mice using a telemetry system. *Brain Res. Brain*
792 *Res. Protoc.* 14, 154–164.
- 793 Williams, P.A., Wuarin, J.P., Dou, P., Ferraro, D.J., Dudek, F.E., 2002.
794 Reassessment of the effects of cycloheximide on mossy fiber
795 sprouting and epileptogenesis in the pilocarpine model of
796 temporal lobe epilepsy. *J. Neurophysiol.* 88, 2075–2087.
- Williams, P.A., Hellier, J.L., White, A.M., Staley, K.J., Dudek, F.E., 797
2007. Development of spontaneous seizures after experimental 798
status epilepticus: implications for understanding 799
epileptogenesis. *Epilepsia* 48 (Suppl 5), 157–163. 800
- Woldbye, D.P., Larsen, P.J., Mikkelsen, J.D., Klemp, K., Madsen, 801
T.M., Bolwig, T.G., 1997. Powerful inhibition of kainic acid 802
seizures by neuropeptide Y via Y5-like receptors. *Nat. Med.* 803
3, 761–764. 804
- Wuarin, J.P., Dudek, F.E., 1996. Electrographic seizures and new 805
recurrent excitatory circuits in the dentate gyrus of 806
hippocampal slices from kainate-treated epileptic rats. 807
J. Neurosci. 16, 4438–4448. 808
- Zappone, C.A., Sloviter, R.S., 2004. Translamellar disinhibition in 809
the rat hippocampal dentate gyrus after seizure-induced 810
degeneration of vulnerable hilar neurons. *J. Neurosci.* 24, 811
853–864. 812

UNCORRECTED PROOF